Crimson Publishers
Wings to the Research

Research Article

Mineralogical and Geochemical Assessment of Monazite, Ilmenite and Zircon in Recent Coastal Black Sands of Uruguay using SEM/EDS Microanalysis

ISSN: 2578-0255

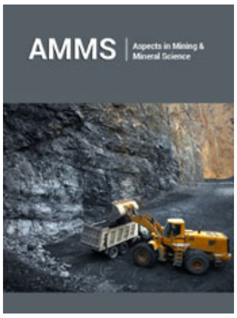

Gonzalo Blanco*, Paulina Abre and Camila Zunino

Department of Geosciences, Eastern Regional University Center, University of the Republic, Uruguay

***Corresponding author:** Gonzalo Blanco, Department of Geosciences, Eastern Regional University Center, University of the Republic, Route 8km 282, Treinta y Tres, Uruguay

Submission: July 11, 2026
Published: July 24, 2026

Volume 15 - Issue 2

How to cite this article: Gonzalo Blanco*, Paulina Abre and Camila Zunino. Mineralogical and Geochemical Assessment of Monazite, Ilmenite and Zircon in Recent Coastal Black Sands of Uruguay using SEM/EDS Microanalysis. Aspects Min Miner Sci. 15(2). AMMS. 000859. 2026.
DOI: 10.31031/AMMS.2026.15.000859

Abstract

This work describes the mineralogical and geochemical features of the heavy mineral assemblage within a very fine- to medium-grained black sand occurrence along the Uruguayan Atlantic coast. Mineralogical analysis focused on the valuable heavy minerals' varieties bearing TiO_2, LREE, and ZrO_2 using a SEM/EDS instrument. The total concentration of valuable heavy minerals (ilmenite, zircon, and monazite) increases from 21% in the raw black sand sample to 65% after concentrating and sieving within the very fine to fine grain-size fraction (63 to 180µm). This concentrated fraction comprises 46% ilmenite, 19% Ti-magnetite, 2% leucoxene and rutile, 5% monazite, and 14% zircon, alongside other non-valuable heavy minerals and light minerals (gangue). Average geochemical microanalysis (n=557) show that the ilmenites are composed of 54% TiO_2, 42% FeO, 1.6% MnO and 0.9% MgO. Ti-magnetites are composed of 36% TiO_2, 58% FeO, 0.7% MnO, 1.8% MgO, 0.7% Al_2O_3, 0.9% SiO_2 and 1.1% CaO. Ce-monazite yields 35% CeO_2, 15.5% La_2O_3, 13.2% Nd_2O_3, 8.8% Th_2O, 1.3% U_3O_8, and 25.7% P_2O_5. Zircon is composed of 65.6% ZrO_2 and 33.1% SiO_2.

Keywords: SEM-EDS; Mineralogy; Geochemistry; Black sands; Ilmenite; Monazite; Uruguay

Introduction

Natural heavy mineral concentration in black sand occurs through eolian, fluvial and wave action in both recent and ancient sedimentary deposits [1,2]. Coastal placer deposits containing ilmenite (Fe_2+TiO_3), leucoxene (an alteration product with >70% of TiO_2), and rutile (TiO_2) represent the main economic source of titanium, accounting for approximately, 45% of known worldwide resources [1,3,4]. When coastal placer deposits additionally accumulate other valuable heavy minerals such as monazite ((Ce,La,Nd,Th)PO_4) and zircon ($ZrSiO_4$), they may be profitable as co- or by-products [1]. Monazite is exploited for its Light Rare Earth Elements (LREE) and thorium (Th) content as a by-product during titanium and zirconium extraction from coastal deposits, such as those in South Africa, Australia, Brazil and India [1,3-8]. Monazite deposits hosting Rare Earth Elements (REEs) are critical raw materials of high economic value [9,10] and strategic relevance globally [1].

Along the Atlantic coast of Uruguay (Figure 1), research on black sand deposits has focused on reserve estimations for potential titanium exploitation, aimed at the production of white and highly opaque TiO_2 pigment [11-13]. However, a significant knowledge gap persists regarding detailed single-grain mineralogical and geochemical analytical data for valuable heavy minerals such as ilmenite, monazite, and zircon. Consequently, the precise chemical variations and potential economic viability of these sub-products remain unresolved.

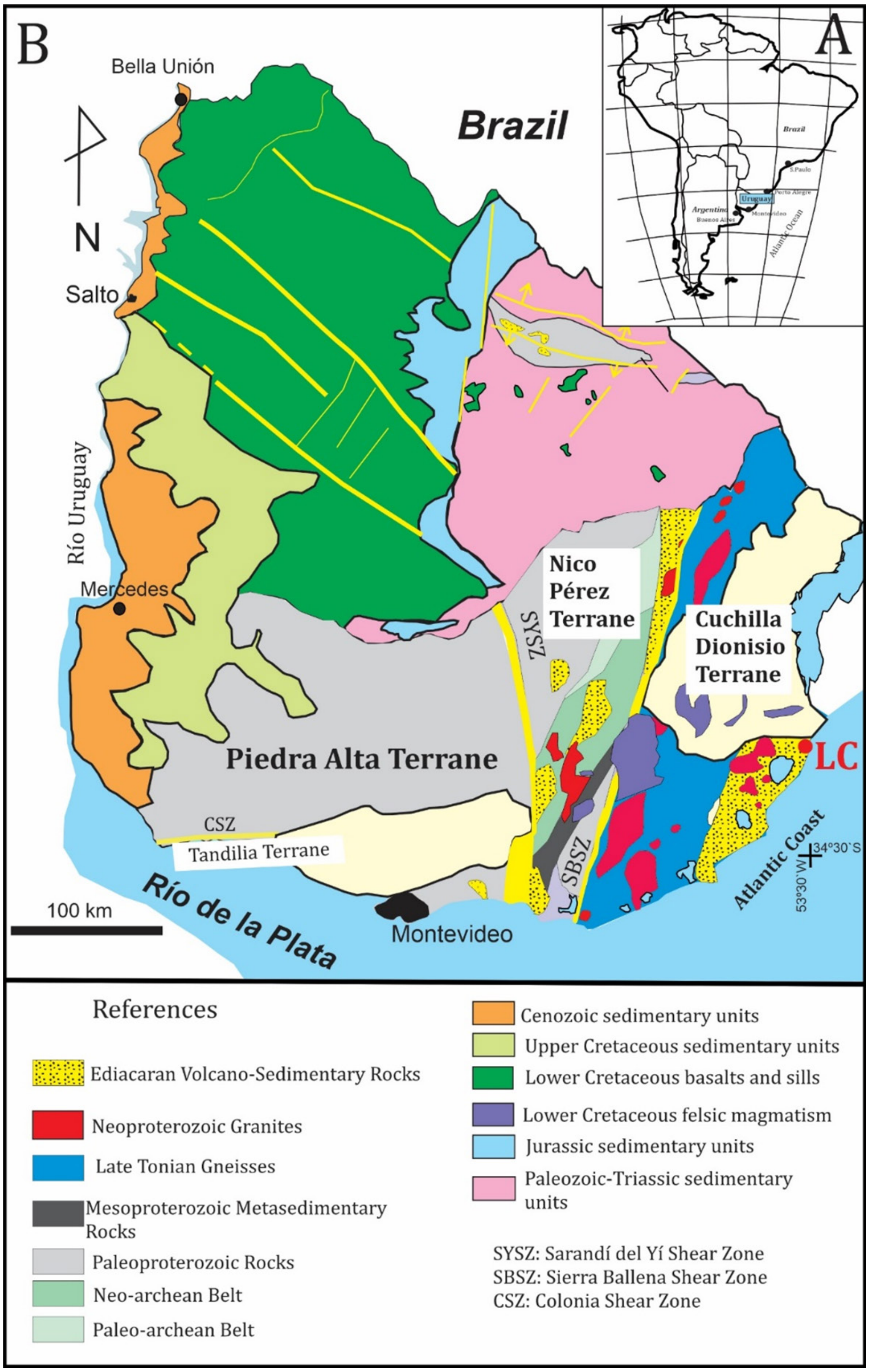

Figure 1: A. Location of Uruguay. B: Simplified Uruguayan geological map, modified after [9,10]. LC: La Coronilla. Paleoproterozoic is misspelled in the references. The letters A are too small to read.

Scanning Electron Microscopy (SEM) coupled with Energy-Dispersive X-ray Spectrometry (EDS) has emerged as a robust, non-destructive, and efficient tool for the characterization of heavy minerals [2] and other aspects of the mining industry [14,15]. Unlike traditional bulk geochemistry methods, SEM-EDS single-grain analysis combined with automated elemental mapping allows precise determination of compositional variations. Furthermore, the technique is useful for identifying internal textures within individual mineral phases, which may influence the economic evaluation and metallurgical processing potential of potential placers and other ores [15].

In this study, we investigate the recent black sand deposits of La Coronilla beach, located approximately 30Km southwest of the Brazilian border. In this area, heavy minerals are concentrated by eolian and wave action and are distributed along the coast, overlying the Late Pleistocene marine sediments of the Chuy Formation. The objective of this work is to evaluate the use of the Scanning Electron Microscopy and Energy-dispersive X-ray spectrometry analysis [16] to characterize the geochemical composition and textural features of valuable economic minerals (ilmenite, monazite, and zircon) and the associated gangue minerals within this coastal system.

Materials and Methods

A 10kg bulk sample was collected from swash zone of the La Coronilla locality in the Atlantic coast of Uruguay. Sample processing and analysis were carried out at the Laboratorio de Geología (Departamento de Geociencias, Centro Universitario Regional del Este) following established procedures [17]. The raw sample was split by quartering, and an aliquot was taken for grain-size separation. Sieving was performed using a Retsch AS 200 analytical sieve shakers to separate four distinct grain-size fractions: 63-125µm, 125, and 180µm and >180µm. A raw black sand aliquot (N) was kept untreated for comparison with the separated mineral fractions. For each fraction, an epoxy resin probe of 1.25-inch diameter was performed. The obtained resin discs were polished with diamond paste of 3µm, 1µm and 1/4µm to obtain a mirror-like finished surface. Subsequently, the mounts were carbon-coated for SEM observations and chemical analysis. Back-Scattered Electron (BSE) imaging and elemental analysis were conducted using a JEOL NeoScope JCM-6000 Plus equipped with an Energy-Dispersive X-ray Spectrometer (EDS) consisting of a 10mm^2 Silicon Drift Detector (SDD). A total of 557 single-grains analyses of major and minor elements were done following standard procedures [18]. Electrons are emitted by a traditional W cartridge filament with a working distance of 19mm. The X-ray take-off angle is about 25°. The energy resolution of the SDD is ~133eV at the energy of Mn Kα (5894eV). The EDS analyses were conducted using standard probe current (~30nA), a data collection time of 60s and an accelerating voltage of 15kv.

Result and Discussion

The modal point-counting results on both the sieved and non-sieved fractions reveal significant trends regarding the selective concentration of valuable heavy minerals (Figure 2). The data confirm that the majority of these valuable mineral phases occur within the 63 to 180µm grain-size range (very fine to fine sand). The 63-125µm and 125-180µm fractions exhibit an exceptionally high concentration of ilmenite (46%), representing a substantial enrichment compared to the >180µm fraction and the raw, non-sieved black sand sample (N), which yields an ilmenite concentration of only 19-21%. Zircon shows concentration levels of 14% and 9% in the 63-125µm and 125-180µm fractions respectively. Monazite preferentially concentrate up to 4-5% within the same 63-180µm size range. In contrast, the primary silicate gangue, quartz, is notably scarce in these very fine to fine fraction, accounting for only 1 and 9% of the 63-125µm and 125-180µm fractions, respectively. However, quartz reaches up to 47% in the raw black sand sample, typically displaying a grain size larger than 180µm.

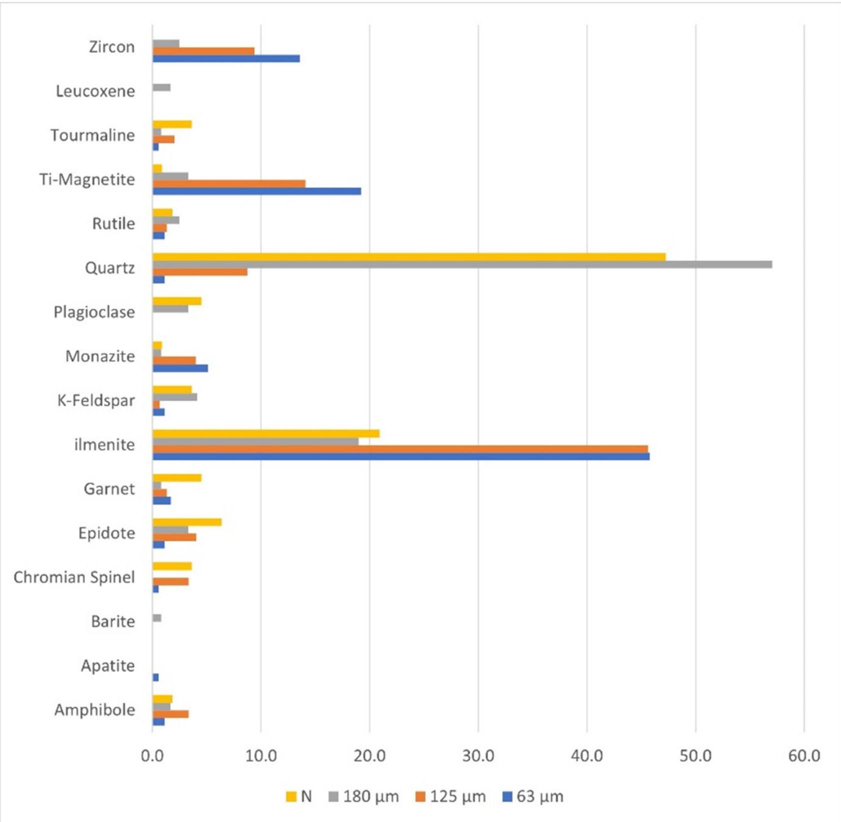

Figure 2: Bar diagram showing the modal mineralogy of heavy mineral phases distributed according to the grain-size. N: raw black sand sample (n=557). I think the letters in the diagram could be bigger.

To validate the modal mineral counts and grain-size distribution, automated elemental mapping and bulk elemental analyses were conducted (Figure 3). Non-valuable heavy minerals such as epidote, amphibole, chromian spinel, tourmaline and garnet account for up to 20% of the total heavy minerals in the raw black sand sample and 14% in the 125-180µm fraction. In contrast, they only constitute up to 5% in the finest fraction (63125µm). Bulk geochemical data (Table 1) strongly support these modal counts, indicating a TiO_2 concentration of approximately 37 wt.% for the fine fractions 63-125µm), compared to around 11wt% in the raw black sand sample. Consequently, sieving the La Coronilla black sands to isolate the very fine to fine grained fractions proves to be a highly effective pre-concentration technique for ilmenite, monazite, and zircon which combined represent up to 65% of the economically valuable heavy minerals.

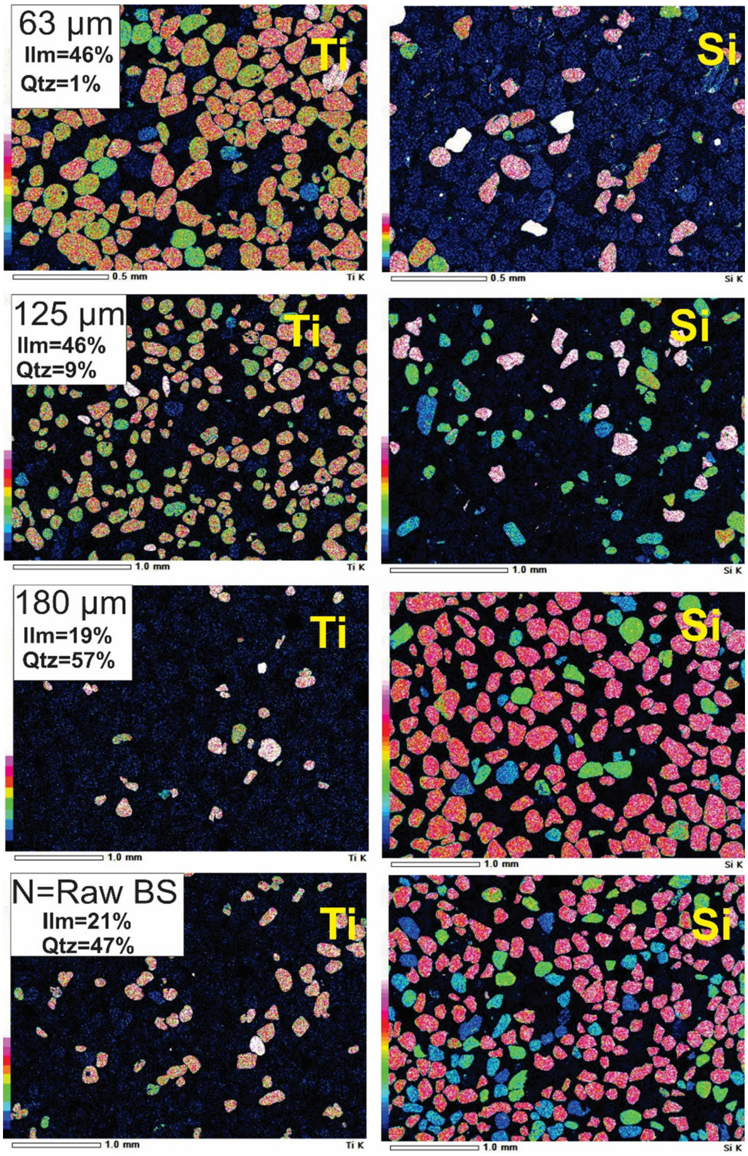

Figure 3: Elemental Ti and Si chemical mapping of the analyzed black sand sample, the efficient removal of quartz (gangue) and the high concentration of ilmenite after sieving. The pink-colored grains within the 63125µm fractions correspond to zircon grains.

Table 1: Average geochemical composition of the analyzed samples taken from the compositional map X-ray spectra. n.d.=no data.

	63µm	125µm	180µm	N
Oxides	% in Weight			
Na_2O	0.44	0.41	0.71	0.71
MgO	1.28	1.21	0.17	0.53
Al_2O_3	3.84	4.29	3.18	6.97

SiO_2	13.24	17.48	85.91	67.35
P_2O_5	1.03	1.1	n.d.	n.d.
K2O	0.06	0.08	0.25	0.45
CaO	1.11	1.14	1.37	2.06
TiO_2	37.67	37.59	4.09	10.83
Cr_2O_3	0.46	n.d.	0.02	0.29
MnO	0.82	n.d.	0.07	0.31
FeO	35.13	33.35	3.58	9.45
ZrO_2	4.93	3.33	0.66	1.04
Total	100	100	100	100

Textural analysis of the ilmenites and Ti-magnetite's indicates that they consist of fine-grained, well-rounded grains. Significant variety in internal textures was observed via Back-Scattered Electron (BSE) imaging (Figure 4). Several ilmenite grains exhibit internal textures, with domains of variable TiO_2 concentrations and inclusions of feldspar, titanite, quartz and zircon (Figure 4). Alteration to leucoxene was also observed, characterized by Ti-rich zones or alteration halos. Monazite and zircon grains are generally texturally homogenous, hosting rare inclusions of quartz or apatite. Single-grain geochemical microanalysis corroborated these mineralogical compositional heterogeneities in ilmenite and variations in the TiO_2 distribution in other mineral phases particularly within Ti-magnetites. Only few grains of rutile and leucoxene were detected and are insignificant economic value in this deposit (Figure 5a). Figure 5b illustrates a trend toward MgO enrichment in the Ti-magnetites, whereas Figure 5c shows elevated MnO concentrations in the ilmenites. On average, ilmenites are composed of 54% TiO_2, 42% FeO, 1.6% MnO, and 0.9% MgO. Ti-magnetites are composed of 36% TiO_2, 58% FeO, 0.7% MnO, 1.8 of MgO, 0.7% Al_2O_3, 0.9% SiO_2, and 1.1% CaO (Table 2). Ce-monazite grains, which reach up to 4-5% within the 63-180µm fractions yield average compositions of 35% CeO_2, 15.5% La_2O_3, 13.2% Nd_2O_3, 8.8% Th_2O, 1.3% U_3O_8, and 25.7% P_2O_3. ThO_2 values show wide dispersion, with concentrations ranging between 3 and 25% (Figure 6). Zircon grains are composed of 65.6% ZrO_2 and 33.1% SiO_2, with negligible trace amounts of LREEs, Th, and Hf.

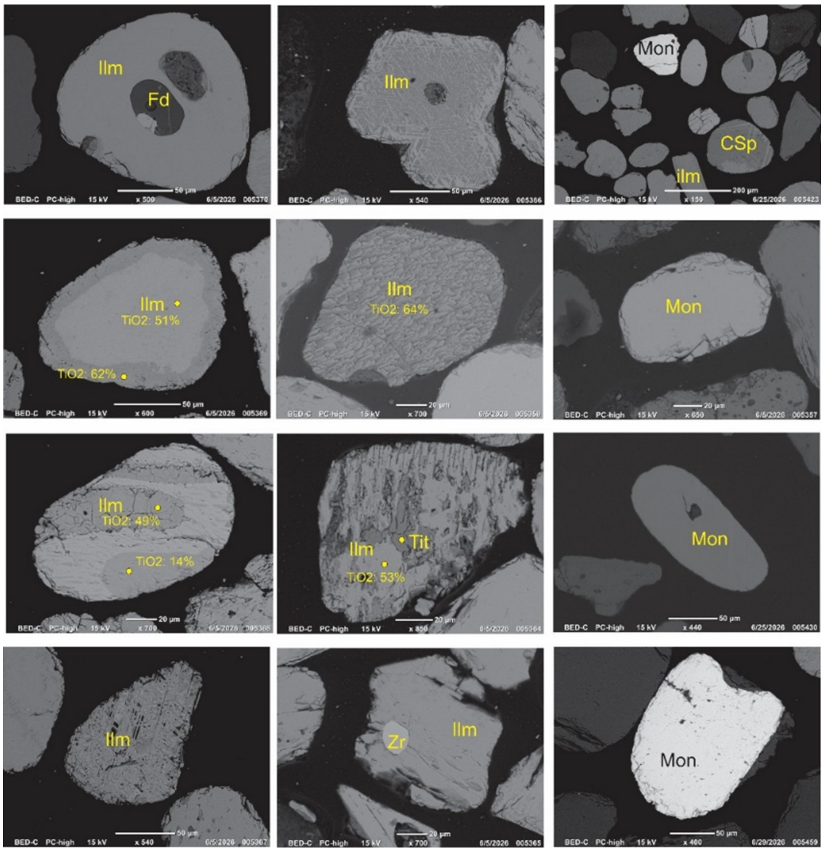

Figure 4: Back-scattered electron images of some analyzed heavy minerals. Ilm: ilmenite, Mon: Monazite, Tit: Titanite, Zr: Zircon, Fd: Feldspar, CSp: Chromian Spinel. Notice the differences in ilmenite textures, inclusions and compositions.

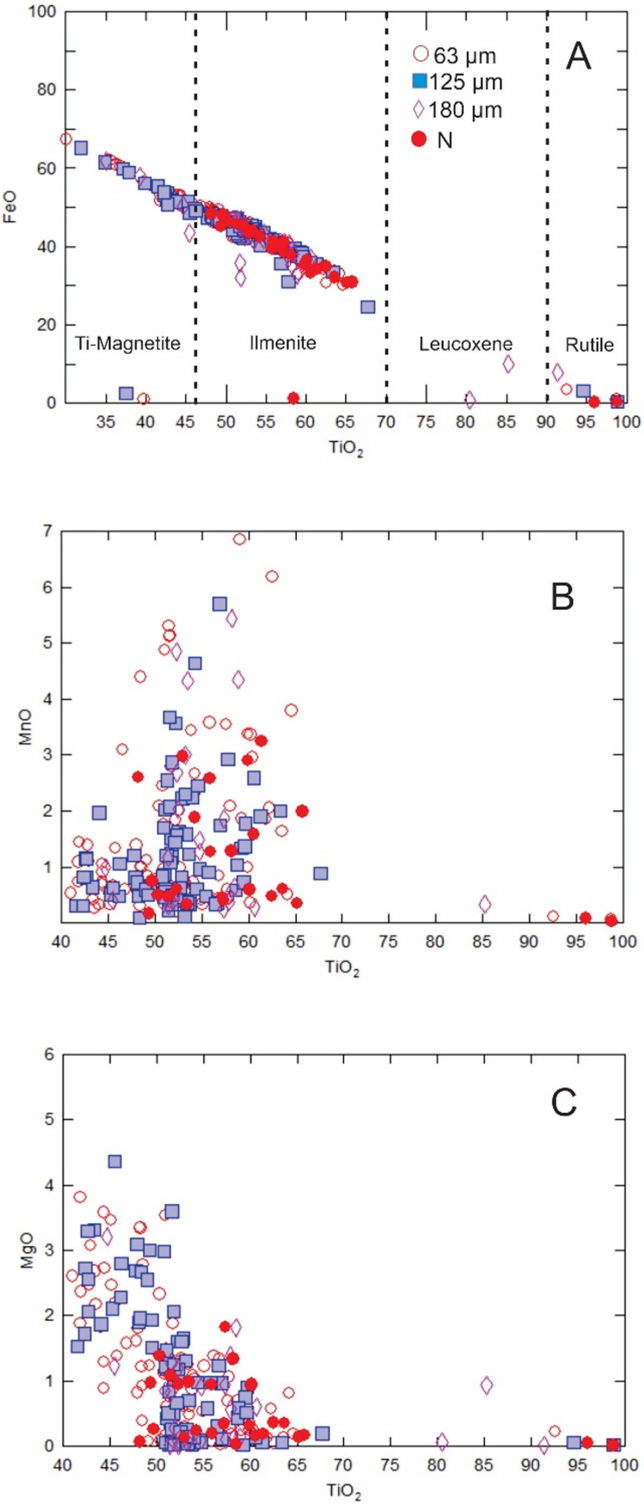

Figure 5: Binary plots characterizing the TiO_2-bearing mineral phases of the black sands, A: TiO_2 vs. FeO, B: TiO_2 vs. MnO and C: TiO_2 vs. MgO. The letters in the diagrams need to be larger.

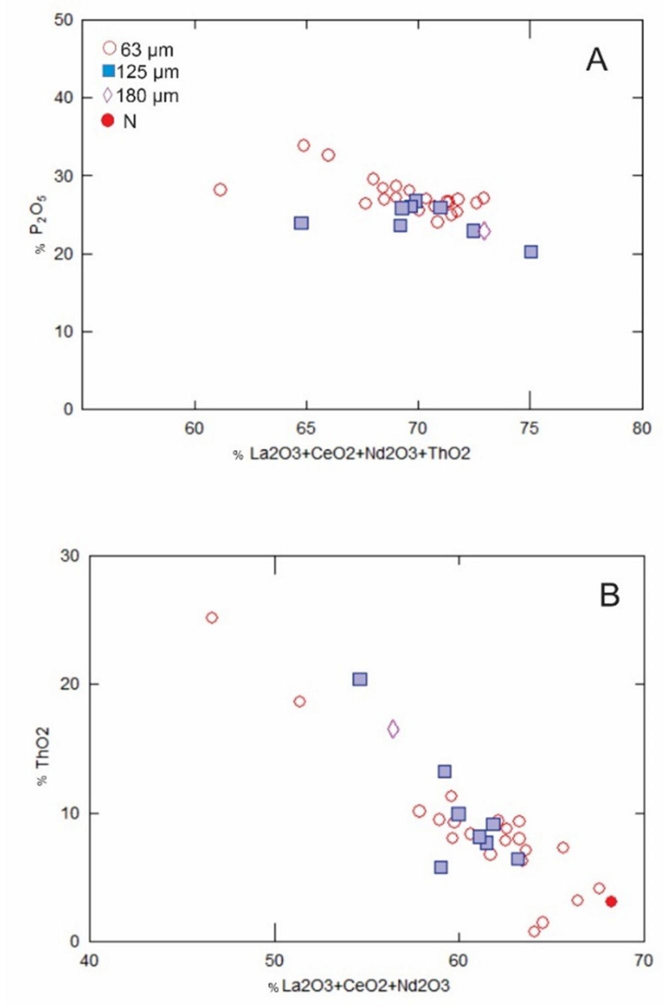

Figure 6: Binary geochemical plots for the analyzed single-grain monazites. A: Total LREE+Th vs. P_2O_5, B: ThO_2 vs. LREE. The letters in both diagrams need to be larger.

Table 2: Average composition of the black sand analyzed minerals.

	Na_20	MgO	$A1_20_3$	$Si0_2$	P_20_5	K_20	CaO	$Ti0_2$	Cr_20_3	Mn0	FeO	$Zr0_2$	La_20_3	$Ce0_2$	Nd_20_3	$Th0_2$	U_30_8
Mineral	% in Weight of Oxides																
Amphibole (n=11)	1.4	9.8	16.2	44.8	0.3	0.7	8.5	4.0	0.1	0.2	14.1						
Cr-Spinel (n=10)	0.2	13.2	20.7	1.2	0.0	0.2	0.2	4.8	30.5	1.0	29.1	0.1					
Epidote (n=19)	0.1	0.1	23.2	39.1	0.1	0.1	23.7	0.2	0.1	0.3	13.0						
Garnet (n=11)	0.1	7.5	21.1	38.1	0.2	0.0	3.4	0.2	0.1	2.5	27.4						
Ilmenite (n=195)	0.1	0.9	0.4	0.3	0.1	0.0	0.4	54.0	0.1	1.6	42.4	0.1					
K-Feldspar (n=12)	1.8	0.5	16.6	69.8	0.0	10.1	0.2	0.2	0.1	0.0	1.1	0.0					
Monazite (n=34)	0.3	0.2	1.6	2.0	25.7	0.2	1.3	1.0	0.1	0.1	8.1		15.5	35.0	13.2	8.8	1.3
Plagioclase (n=9)	6.8	0.1	24.5	60.2		0.4	7.1	0.1	0.0	0.0	0.7						
Quartz (n=136)	0.1	0.0	0.3	98.7		0.0	0.1	0.1	0.1	0.1	1.0						
Rutile (n=7)	0.1	0.1	0.6	0.7	0.1	0.1	0.1	95.9	0.1	0.1	2.3						
Ti-Magnetite (n=68)	0.1	1.8	0.7	0.9	0.1	0.0	1.1	36.1	0.1	0.7	59.0	0.2					
Tourmaline (n=9)	0.1	1.7	54.1	28.4	0.2	0.0	0.0	0.6	0.1	0.1	14.8						
Leucoxene (n=2)	0.2	0.5	1.3	9.3		0.1	0.2	82.9	0.2	0.3	5.3						
Zircon (n=41)	0.1	0.1	0.4	33.1		0.0	0.1	0.2	0.1	0.1	0.3	65.6					

Furthermore, others valuable heavy mineral like manganocolumbite (Mn, Fe^{2+}) $(Nb,Ta)_2O_6$ and xenotime $Y(PO_4)$ grains were detected in the black sands but they are scarce and thus, further investigation is needed to evaluate these minerals from an economic perspective (Figure 7). The granulometric separation applied in this study highlights an increase in total valuable heavy minerals (ilmenite-zircon-monazite), rising from 21% in the raw black sand sample to 65% within the very fine to fine grained fraction. A similar heavy mineral concentration in the finest fraction was previously documented in the Aguas Dulces black sand deposit near La Coronilla beach [12]. However, the LREE reserve calculation for the Aguas Dulces deposit was limited because single-grain geochemical analyses on monazite were not conducted, and the ΣLREE was unreported. In this work, the analyzed monazites yielded an outstanding average of 64% ΣLREE (n=35, standard deviation of 8%). This high value, combined with the proven capability to concentrate this mineral up to 5% via sieving within the 63-180µm range, highlights the need for further research to reevaluate the reserves of this strategic resource along the Uruguayan coast. From a processing standpoint, the sharp compositional and granulometric boundary between the valuable heavy minerals and the identified gangue (quartz), offers a favorable scenario for low-cost gravimetric or magnetic separation.

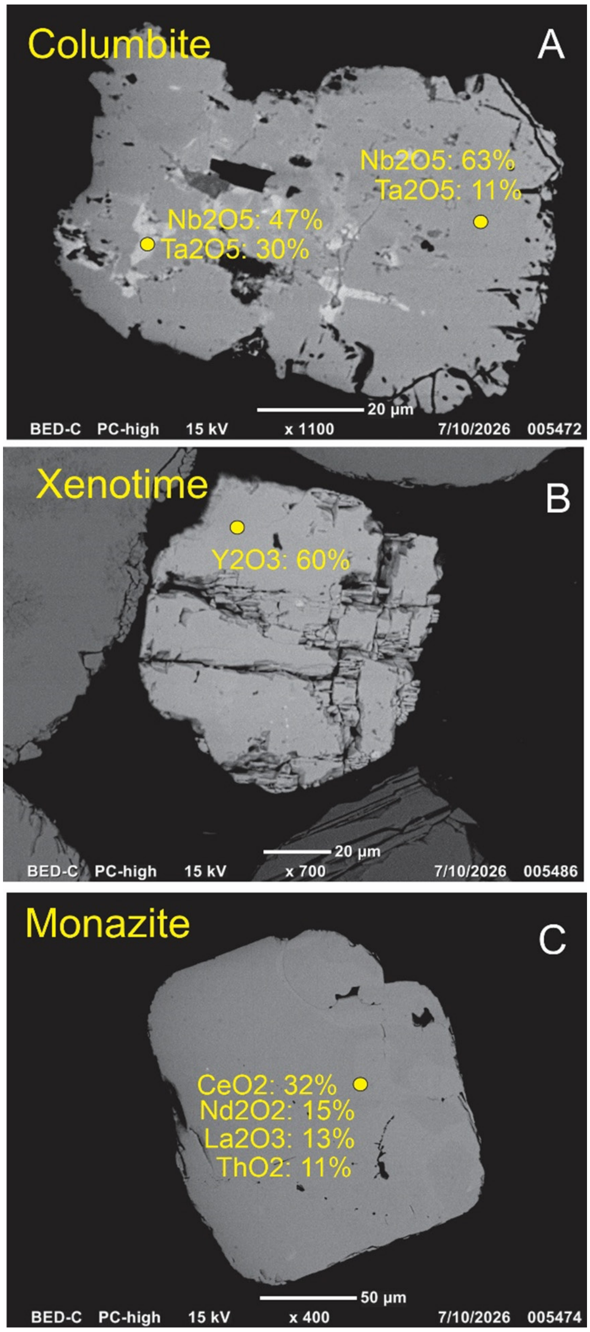

Figure 7: Back-scattered electron images of valuable heavy minerals founded the very fine to fine sand fractions (63-180µm). Only two grains of columbite and xenotime were detected.

Conclusion

The integration of the Scanning Electron Microscopy (SEM) and Energy-Dispersive X-ray Spectrometry (EDS), combined with modal point counting and geochemical mapping, provides a powerful approach for characterizing the mineralogical and geochemical features of coastal placer deposits. At La Coronilla beah, a simple granulometric separation effectively isolates the economically important phases. The very fine to fine sand fractions (63-180μm) selectively concentrate 65% of the valuable heavy minerals dominated by ilmenite, monazite, and zircon. the majority, which consist of Ilmenite yields an average TiO_2 composition of 54% with a standard deviation of 4%. Although individual leucoxene grains as alteration products are scarce, some ilmenite and Ti-magnetite grains show varying degrees of alteration, characterized by Ti-rich zones and halos. Ce-monazite and zircon grains are homogenous, rounded and very fine to fine grained. Monazite are composed of 64% LREE (standard deviation of 8%), whereas lastly, zircon grains are composed of 65.6% ZrO_2.

Acknowledgement

The authors are grateful to the Universidad de la República and PEDECIBA Geociencias for their support. The reviewers and the Editor are deeply acknowledged.

References

1. Pohl WL (2005) Economic Geology. Blackwell Scientific Publications, Oxford, p. 663.
2. Blanco G, Abre P, Rajesh HM, Germs GJB (2014) Geochemistry and heavy minerals analyses on “black sands” of the lower Cambrian Fish River Subgroup (Nama Group, Namibia). South African Journal of Geology 117(1): 129-148.
3. Fockema PD (1986) The heavy mineral deposits north of Richards Bay. In: Anhaeusser CR, Mask S (Eds.), Mineral deposits of Southern Africa. Geol Soc S Afr, Johannesburg, pp. 2301-2307.
4. Hamilton NTM, Collins LB (1998) Placer formation in a Holocene barrier system, Southwestern Australia. J Coast Res 14: 240-255.
5. Roy PS (1999) Heavy mineral beach placers in Southeastern Australia: Their nature and genesis. Econ Geol 94(4): 567-588.
6. Knundsen K, McLimans RK (1998) TiO_2 in coastal sands of Brazil. Geological Survey of Denmark and Greenland (GEUS), p. 57.
7. Dillenburg SR, Tomazelli LJ, Barboza EG (2004) Barrier evolution and placer formation at Bujuru southern Brazil. Marine Geology 203(1-2): 43-56.
8. Peristeridou E, Melfos V, Papadopoulou L, Kantiranis N, Voudouris P (2022) Mineralogy and mineral chemistry of the REE-rich black sands in beaches of the Kavala District, Northern Greece. Geosciences 12: 277.
9. Blanco G, Abre P, Ferrizo H, Gaye M, Gamazo P, et al. (2021) Revealing weathering, diagenetic and provenance evolution using petrography and geochemistry: A case of study from the Cretaceous to Cenozoic sedimentary record of the SE Chaco-Paraná basin in Uruguay. J S Am Earth Sci 105: 102974.
10. Bossi J, Ferrando L (2001) Geological Map of Uruguay at 1:500,000 scale, digital version 2.0. Faculty of Agronomy, Montevideo, Uruguay.
11. Bossi J, Navarro R (2000) Recursos Minerales del Uruguay. ISBN9974 39 281 0 Montevideo, Uruguay, p. 416.
12. Soares de Lima C, Preciozzi F, Medina E (2002) Black sand deposit at Aguas Dulces, Rocha Department. Directorate of Mining and Geology, p. 169.
13. Ferrando L, Bossi J, Maldonado S, Schipilov A, Campal N (2003) Evaluation of black sand reserves in Aguas Dulces, Rocha Department, Uruguay. Journal of the Geological Society of Uruguay 10: 15-28.
14. Flude S, Haschke M, Storey M (2017) Application of benchtop micro-XRF to geological materials. Mineralogical Magazine 81(4): 923-948.
15. Blanco G, Abre P, Zunino C, Mármol S (2026) SEM-EDS microanalysis of sedimentary and felsic volcanic units in Uruguay: A new analytical approach for pozzolanic resource assessment. Aspects in Mining & Mineral Science 15(1): 1833-1839.
16. Blanco G, Tarjan I, Abre P, Zunino C, Segovia D (2025) SEM and EDS mineral analysis of the cerro papagayo iron- manganese deposit from Uruguay. Journal of Mineral Science and Materials 6: 1121.
17. Abre P, Blanco G (2026) Laboratory workflows for integrated provenance analyses. International Journal of Innovative Research in Science Engineering and Technology 15(5): 7431-7438.
18. Chen Y, Chen Y, Liu Q, Liu Xi (2023) Quantifying common major and minor elements in minerals/rocks by economical desktop scanning electron microscopy/silicon drift detector energy-dispersive spectrometer (SEM/SDD-EDS). Solid Earth Sciences 8(1): 49-67.